Phase Diagram of Electronic Models for Transition Metal Oxides in One Dimension

Jose Riera,[1] Karen Hallberg,[2] and Elbio Dagotto[3]
[1]*Instituto de Física Rosario y Depto. de Física, Universidad Nacional de Rosario, 2000 Rosario, Argentina*
[2]*Max-Planck-Institut für Physik Komplexer Systeme, Bayreuther Strasse 40, D-01187 Dresden, Germany*
[3]*Department of Physics and National High Magnetic Field Lab, Florida State University, Tallahassee, Florida 32306*
(Received 20 August 1996)

The zero temperature phase diagram of the ferromagnetic Kondo model in one dimension is studied using numerical techniques, especially at large Hund coupling. A robust region of fully saturated ferromagnetism (FM) is identified at all densities. Phase separation between hole-rich and hole-poor regions and a paramagnetic regime with quasilocalized holes were also observed. It is argued that these phases will also appear in two and three dimensions. Our results apply both to manganites and one-dimensional compounds such as $Y_{2-x}Ca_xBaNiO_5$. As the transition metal ion spin grows, the hole mobility rapidly decreases, explaining the differences between Cu oxides and Mn oxides. [S0031-9007(97)03668-5]

PACS numbers: 71.10.Pm, 75.10.–b, 75.30.Kz

Doping of transition metal oxides (TMO) with perovskite structure induces remarkable phenomena such as high temperature superconductivity, charge ordering, and anomalous transport properties. Typical examples are the layered Cu oxides and Ni oxides. Recently, another dramatic property of doped TMO has been revealed: at low temperature (T) $La_{1-x}Ca_xMnO_3$ changes from an antiferromagnetic (AF) insulator to a FM metal as x grows from 0. "Colossal" magnetoresistance is observed in this compound [1]. At the critical FM temperature, a metal-insulator transition occurs. At larger doping $x > 0.5$, a charge-ordered AF state was detected [2].

The double exchange mechanism has been used to explain the FM phase in Mn oxides [3,4]. However, recent reexamination of the double exchange model revealed that electrons can collect a Berry phase that may induce low energy states in the spectrum [5]. Also, recent experiments have shown that the dynamical properties of the ferromagnetic phase are nontrivial [6]. The combination of these results and the complicated experimental phase diagram of manganites [2] suggest that electronic models more realistic than the double exchange model may have a phase diagram richer than expected, which deserves to be studied with state-of-the-art computational techniques. Such studies would clarify, among other issues, whether FM indeed exists in the $T = 0$ ground state, and especially what phases are in competition with it. In addition, it would be important to analyze the origin of the drastic differences between Cu oxides and Mn oxides regarding their doped-induced properties. The cuprates have metallic and superconducting phases, while the manganites are either charge-ordered insulators or ferromagnets [2]. In this Letter, all these issues are addressed.

The Hamiltonian widely used for Mn oxides is [3,4]

$$H = -t \sum_{\langle \mathbf{mn} \rangle \sigma} (c^{\dagger}_{\mathbf{m}\sigma} c^{\dagger}_{\mathbf{n}\sigma} + \text{H.c.}) - J_H \sum_{\mathbf{n}} \boldsymbol{\sigma}_{\mathbf{n}} \cdot \mathbf{S}_{\mathbf{n}} . \tag{1}$$

Here the first term represents the e_g-electron transfer between nearest-neighbor Mn ions at sites $\mathbf{m}$ and $\mathbf{n}$. The second term corresponds to the Hund coupling ($J_H > 0$) between the $S = 3/2$ t_{2g} localized spin $\mathbf{S}_{\mathbf{n}}$ and the spin $\boldsymbol{\sigma}_{\mathbf{n}}$ of the mobile e_g electron at the same site. Coulombic repulsion in the e_g band is not included in Eq. (1), but it is considered in some calculations below. Phenomenologically, it is expected that $J_H \gg t$, which favors the alignment of the itinerant and localized spins. For Mn^{3+}, where the e_g level is occupied, the resulting spin is 2, while for Mn^{4+} (vacant e_g state) the spin is 3/2. Thus, at $J_H = \infty$ the effective degrees of freedom become $S = 2$ "spins" and $S = 3/2$ "holes" which is the language convention followed below. In this limit Eq. (1) reduces to a simpler hole-hopping Hamiltonian. For "spin" values $S \geq 1$, the hopping term at $J_H = \infty$ is [5]

$$H_{J_H=\infty} = -t \sum_{\langle \mathbf{mn} \rangle} P_{\mathbf{mn}} Q_S(y) , \tag{2}$$

where $y = \mathbf{S}_{\mathbf{m}} \cdot \mathbf{S}_{\mathbf{n}}/S(S - 1/2)$, and for Mn oxides ($S = 2$) the polynomial $Q_S(y)$ is $Q_2(y) = -1 - \frac{5}{4}y + \frac{7}{4}y^2 + \frac{3}{2}y^3$. For Ni oxides ($S = 1$) $Q_1(y) = (1 + y)/2$ [7]. Hamiltonian Eq. (2) is rotational invariant, and it acts only on links containing one spin and one hole. $P_{\mathbf{mn}}$ permutes the hole and the spin. The $\mathbf{S}_{\mathbf{n}}$ operators are standard, and in Eq. (2) they act over both the spin and hole involved in the hopping process; i.e., the kinetic terms not only interchange their site positions, but they can flip their spin projections as well [5,7]. This is an important difference with respect to the t-J model for cuprates. At large but finite J_H, Eq. (2) is supplemented by a Heisenberg interaction between nearest-neighbor spins of the form $J \sum_{\langle \mathbf{mn} \rangle} (\mathbf{S}_{\mathbf{m}} \cdot \mathbf{S}_{\mathbf{n}} - n_{\mathbf{m}} n_{\mathbf{n}}/4)$, in the standard notation [8]. This term affects only the S spins since in hole states the orbital with mobile electrons (e_g) is empty. Phonons are not considered in the present study. Although their importance is clear in some experiments

[9], we consider it worthwhile to study the electronic sector in isolation. The rich phase diagrams found here justify such an approach.

Experience with Cu oxide models have shown that the analysis of Hamiltonians in 1D chains [10] can provide important insight on qualitative features of the phase diagram that also exist in the realistic dimension $D = 2$ [8]. Since 1D is the best for numerical techniques, our study below is restricted to chains [11] and complements work in the other extreme case $D = \infty$ [4]. Thus, the goal of the present paper is not to establish quantitative predictions for 3D TMO, a quite hard task, but to search for qualitative features of the 1D phase diagram that may survive the increase in dimensionality. Note also that the special case $S = 1$ and 1D has intrinsic relevance since the compound $Y_{2-x}Ca_xBaNiO_5$ with NiO chains has been recently synthesized [12]. The same compound but with Co replacing Ni can also be prepared [13]. Thus, our study is of importance for materials beyond the manganites. As numerical techniques the exact diagonalization [8] (ED) and the density matrix renormalization group [14] (DMRG) methods were used. The special case $S = 1$ will be studied together with the relevant case for Mn oxides ($S = 2$) to observe the effect of different transition metal spins in the phase diagrams.

First, let us consider ferromagnetism. It can be shown that the ground state of Eqs. (1) and (2) in 1D is a fully saturated ferromagnet (FM) for hole density $x \neq 0, 1$ in the case of *open* boundary conditions (OBC) and $J_H = \infty$ (or $J = 0$). The proof is due to Kubo [15]: the matrix elements of the $J = 0$ Hamiltonian Eq. (2) in the standard S^z basis are *nonpositive*, which is shown by explicitly writing the polynomials $Q_s(y)$ in matrix form for a given link. For a subspace with a fixed total spin projection S^z_{total}, this property implies that the ground state is nondegenerate and the coefficients of this state expanded in the S^z basis are of the same sign (Perron-Frobenius theorem). Since in each subspace with a fixed S^z_{total} the state $|S_{\max}, S^z_{\text{total}}\rangle$ with the maximum possible spin $S_{\max}$ also has coefficients of the same sign, then the ground state in such subspace must be the ferromagnetic state. This proof is not valid for *twisted* boundary conditions, including periodic and antiperiodic conditions (PBC and APBC, respectively), since in this case across the boundary it is possible to move fermions from site N to 1 (for a N-site chain), collecting anticommutation signs which make the matrix elements not necessarily negative. For the same reason the proof is not valid in higher dimensions even with OBC. Another important detail is that each S^z_{total} subspace is assumed to be fully connected (i.e., all elements of the basis are reached by successive applications of the Hamiltonian over any of its members). Actually in the 1D *t-J* model, the Hilbert space is disconnected [16] for $J = 0$ and the theorem does not hold. However, if $S \geq 1$ the Hilbert space is *connected* since together with a hopping, the spins and holes can flip their spin projections [17]. This is an interesting conceptual difference between models for cuprates and other TMO's with consequences for ferromagnetism.

Solving exactly Eq. (2) on finite chains with OBC, we verified the existence of ground state FM for any $x \neq 0, 1$. We also observed that using PBC (APBC) for an odd (even) number of holes, i.e., using closed shells, for both $S = 1$ and 2, the ground state at $J = 0$ is again a FM. Thus, to increase the size of the chains that can be studied numerically with ED techniques, preserving the correct properties of the ground state, below closed-shell BC have been used in addition to OBC. Previous studies [11] have shown that these BC are appropriate for bulk properties. On the other hand, using PBC for an even number of holes, the ground state is a spin singlet [18]. This well-known behavior of closed versus nonclosed shells [11] should not confuse the reader since locally the spin correlations are ferromagnetic even with nonclosed-shell BC [18]. Thus, there is no doubt that the model Eq. (1) in 1D at large J_H has a ferromagnetic ground state [19].

In Fig. 1(a) the phase diagram for $S = 1$ is shown. Chains with up to 16 sites were studied with ED. Using the closed-shell BC, a robust region of FM was identified. The FM boundary was also calculated using the DMRG technique at $x = 0.25$, 0.50, and 0.75 with chains of up to 40 sites and OBC [20]. The critical coupling to reach FM

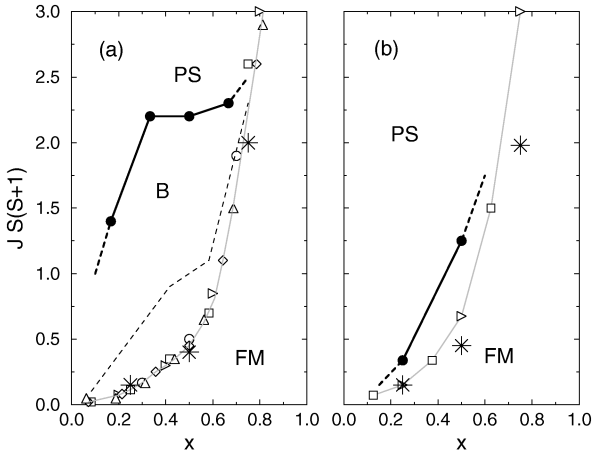

FIG. 1. (a) Phase diagram of the $S = 1$ Hamiltonian Eq. (2) on a 1D chain [$JS(S + 1)$ is the coupling scaled with the spin, x the hole density, and $t = 1$]. The gray line and open points denote the FM phase boundary. Open circles (10), rotated triangles (10), squares (12), diamonds (14), and triangles (16) correspond to ED results using closed-shell BC (in parentheses the number of sites). DMRG results for the FM boundary with OBC and $N = 40$ are also shown (stars). The solid line joining full circles is the phase separation (PS) boundary calculated with ED ($N = 12$). A hole binding (B) region exists between the dashed line and phase separation; (b) same as (a) but for the $S = 2$ Hamiltonian. The boundaries of phase separation and FM were evaluated with ED on chains of $N = 8$ sites. DMRG results on $N = 30$ OBC are shown (stars). In the intermediate metallic region there is binding.

obtained with ED and DMRG are in excellent agreement, showing that size effects are small [21].

Also in Fig. 1(a), regions of phase separation and hole binding have been identified using ED by calculating the compressibility and binding energy from $E(M \pm 2)$, $E(M \pm 1)$, and $E(M)$, where $E(M)$ is the ground state energy for M holes [22]. Phase separation is not contained in the double exchange model, and it occurs when the kinetic energy gained by making holes mobile is overcome by the magnetic energy lost. This has also been observed in the t-J model in both 1D and 2D [8,23]. However, at $x = 0.5$ phase separation appears at $J/t \sim 1.1$, which is much smaller than the coupling $J/t \sim 3.0$ needed in the t-J model [10], suggesting that electronic phase separation may play an important role in the physics of Mn oxides. This issue will be studied in future work carried out in realistic dimensions [24]. Close to phase separation there is a binding region where holes form mobile pairs. Superconductivity is likely in this regime. Finally, note that the $S = 1$ chain has a nonzero spin-gap at half filling. The behavior of holes in such a background has been recently studied [7], where it was observed that in-gap states are created upon doping. Thus, a "spin-gap" regime is not included in Fig. 1(a).

In Fig. 1(b), the $S = 2$ phase diagram is shown. Here the chains accessible to ED (DMRG) have 8 (30) sites. The finite-size effects on the FM line are small. As for $S = 1$, a robust regime of FM has been identified. We observed that the FM lines of Figs. 1(a) and 1(b) are very similar if J is scaled as $JS(S + 1)$. Phase separation and binding are also present. Note that for $S = 2$ the intermediate metallic regime is very narrow; i.e., as S grows the trend observed in Figs. 1(a) and 1(b) suggests that the phase separated and FM phases become dominant. To understand this effect note that the "vaporization" of a large spin cluster in the phase separation region, held together by magnetic forces of effective strength $JS(S + 1)$, can occur only if a substantial gain in kinetic energy, dominated by t, is achieved by the vaporized spins in the hole rich region. Thus, the critical $J/t|_{\mathrm{PS}}$ for phase separation should follow $J/t|_{\mathrm{PS}} \sim 1/S(S + 1)$, or a faster decay with S once the reduction in hole kinetic energy due to the magnetic background is considered. This argument breaks down at very small J/t where the FM state becomes energetically competitive. Thus, in the large S limit the metallic regime at $T = 0$ would disappear in favor of phase separation and FM phases. The arguments presented here do not depend crucially on the dimensionality, and thus a similar behavior is expected in 2D and 3D systems.

The study of the intermediate (paramagnetic) regime is interesting since this phase and the paramagnetic insulator above the critical temperature observed in manganites could be analytically connected. As S grows, a tendency toward localization is indeed observed in the intermediate phase between FM and phase separation in Fig. 1. For example, in Fig. 2(a) the bandwidth W of *one* hole for $S = 1/2, 1$, and 2 vs $t/JS(S + 1)$ is shown. It is clear that W rapidly diminishes with S. The presence of spin gaps in the undoped regime is not fundamental for this behavior since the holes mainly react to the *local* spin environment which is mostly AF even for a $S = 1$ chain [7,25]. Similar effects are observed in Fig. 2(b) where the kinetic energy in the metallic region is presented at $x = 0.5$. Such a mobility reduction is reasonable since holes destroy the magnetic order in their movement, paying an energy that rapidly grows with the spin. The large effective mass for $S = 2$ indicates that small perturbations away from a translational invariant system may localize the carriers. This effect and the dominance of phase separation and FM at large S provides a possible explanation for the notorious experimental differences at low-T between Cu oxides, which show metallic and superconducting phases, and Mn oxides, which have FM and charge-ordered phases [2] (studies in Ni oxides have shown that charge ordering and phase separation are related phenomena [26]).

The Hamiltonian Eq. (1) does not include a spin-spin exchange between the t_{2g} spins since such a coupling arises indirectly from Eq. (1) mediated by the e_g electrons. However, as $x \to 1$ this RKKY coupling vanishes, which is not in agreement with experiments that show AF order at $x = 1$. To remedy this problem phenomenologically, a Heisenberg interaction with coupling J' between the "holes" (which carry spin) can be introduced. At $x = 1$ now the ground state would be AF as for $x = 0$. For completeness, the numerical analysis of Fig. 1(a) was repeated, adding a term $J' \sum_{\langle \mathbf{mn} \rangle} (\mathbf{S_m} \cdot \mathbf{S_n} - n_{\mathbf{m}} n_{\mathbf{n}}/4)$ between the $S = 1/2$ holes and considering $J' = J$ [see

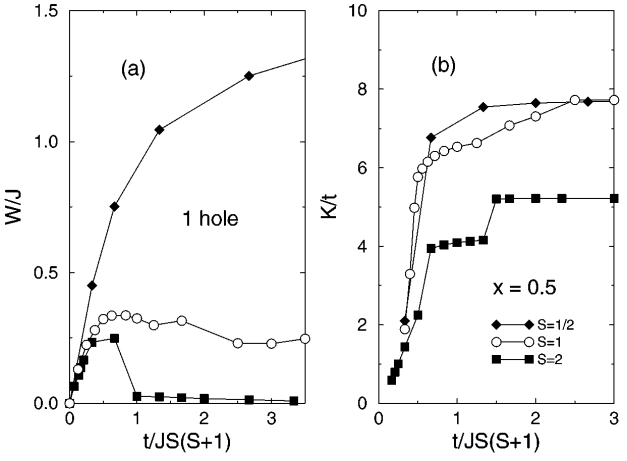

FIG. 2. (a) Bandwidth W/J vs $t/JS(S + 1)$ for *one* hole and $S = 1/2$ (full diamonds), 1 (open circles), and 2 (full squares) calculated using ED techniques on $N = 12, 12$, and 8 chains, respectively. (b) Kinetic energy (hopping term ground state expectation value) in units of t vs $t/JS(S + 1)$ obtained at $x = 0.5$ for $S = 1/2, 1$, and 2 using $N = 12, 12$, and 8 chains, respectively.

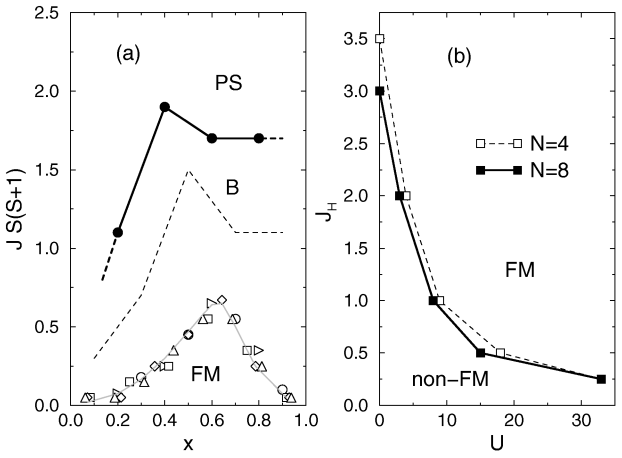

FIG. 3. (a) Same as Fig. 1(a) but adding a Heisenberg interaction between the $S = 1/2$ holes of strength $J'J$. (b) Phase diagram of the Kondo model Eq. (1) at $x = 0.5$, including an e_g Hubbard repulsion of strength U ($t = 1$). Open (full) squares are results obtained with ED (DMRG) on chains with $N = 4$ (8) sites. The non-FM region may have ground state weak ferromagnetism.

Fig. 3(a)]. Up to $x \approx 0.5$ the phase diagram is similar to the results of Fig. 1(a), but as x grows further the coupling needed to reach the FM phase is reduced, as expected.

Finally, in Fig. 3(b) the phase diagram of Eq. (1) solved exactly on a 4-site chain and using DMRG on an 8-site chain, both with OBC and at $x = 0.5$, is shown. Here, an on-site Hubbard repulsion U/t for e_g electrons is incorporated in the Hamiltonian. In agreement with our analysis of the $J_H = \infty$ limit (which suppresses double occupancy as much as a strong on-site Coulomb repulsion), the ground state is FM at large J_H. As U/t grows, FM becomes stable even at small J_H. As with model Eq. (2), the non-FM region contains a weak ferromagnetic component; i.e., for $J_H = U = 1$ and $N = 8$, using DMRG we find spin one in the ground state.

Summarizing, a numerical study of the 1D Kondo Hamiltonian for TMO in the $J_H \gg t$ limit and also at finite J_H has been presented. The phase diagram contains a robust FM region at all densities, contrary to the case of the 1D t-J model for Cu oxides. At finite exchange J, a narrow metallic window with low mobility carriers separates the FM region from a phase-separated regime not contained in the double exchange model. As the spin S grows, phase separation and FM become dominant, the intermediate metallic regime tends to disappear, and the mobility of holes in the non-FM region rapidly decreases. It was argued that the 2D and 3D versions of the Kondo Hamiltonian for manganites should present a similar behavior. Preliminary results support this conjecture [24].

We thank E. Müller-Hartmann, K. Penc, A. Sandvik, and P. Thalmeier for useful conversations. E. D. is supported by the NSF Grant DMR-9520776.

[1] S. Jin *et al.*, Science **264**, 413 (1994).
[2] P. E. Schiffer, A. P. Ramirez, W. Bao, and S-W. Cheong,Phys. Rev. Lett. **75**, 3336 (1995); C. H. Chen and S-W. Cheong, Phys. Rev. Lett. **76**, 4042 (1996).
[3] C. Zener, Phys. Rev. **82**, 403 (1951); P. W. Anderson and H. Hasegawa, Phys. Rev. **100**, 675 (1955); P. G. de Gennes, Phys. Rev. **118**, 141 (1960); J. Inoue and S. Maekawa, Phys. Rev. Lett. **74**, 3407 (1995).
[4] N. Furukawa, J. Phys. Soc. Jpn. **63**, 3214 (1994).
[5] E. Müller-Hartmann and E. Dagotto, Phys. Rev. B **54**, R6819 (1996).
[6] J. W. Lynn *et al.*, Phys. Rev. Lett. **76**, 4046 (1996).
[7] E. Dagotto, J. Riera, A. Sandvik, and A. Moreo, Phys. Rev. Lett. **76**, 1731 (1996).
[8] E. Dagotto, Rev. Mod. Phys. **66**, 763 (1994).
[9] R. H. Heffner *et al.*, Phys. Rev. Lett. **77**, 1869 (1996).
[10] M. Ogata *et al.*, Phys. Rev. Lett. **66**, 2388 (1991).
[11] A similar approach has been used in the context of heavy-fermions [see, e.g., K. Ueda *et al.*, Phys. Rev. B **50**, 612 (1994); M. Sigrist *et al.*, Phys. Rev. B **46**, 175 (1992)].
[12] J. F. DiTusa *et al.*, Phys. Rev. Lett. **73**, 1857 (1994).
[13] R. Cava, private communication.
[14] S. R. White, Phys. Rev. Lett. **69**, 2863 (1992).
[15] K. Kubo, J. Phys. Soc. Jpn. **51**, 782 (1982); see also M. Sigrist *et al.*, Phys. Rev. B **46**, 13 838 (1992).
[16] Y. Nagaoka, Phys. Rev. **147**, 392 (1966).
[17] For example, consider a 3-site OBC problem for $S = 1$ and an initial state $|1/2, -1/2, 1\rangle$ (with numbers representing z-direction spin projections): here four applications of Eq. (2) connect this state with, e.g., $|-1/2, 1/2, 1\rangle$. On the other hand, for the t-J model the states $|1/2, -1/2, 0\rangle$ and $|-1/2, 1/2, 0\rangle$ are disconnected.
[18] J. Zang *et al.* (to be published); see also T. A. Kaplan and S. D. Mahanti, J. Phys.: Condens. Matter **9**, L291 (1997).
[19] Similar boundary dependence of the total spin have been observed in 2D t-J clusters. See A. Barbieri, J. A. Riera, and A. P. Young, Phys. Rev. B **41**, 11 697 (1990).
[20] To find the boundaries of the FM phase with DMRG we compared the energies of different subspaces with fixed S^z_{total}. The FM case is accurate, with a truncation error of 10^{-12} for $N = 100$ when keeping $m = 200$ states per block. The states with smaller S^z_{total} are less precise due to a larger Hilbert space. For $S = 1$ ($S = 2$) we used $m = 200$ ($m = 100$), $N = 40$ (30), with an error 10^{-6} (10^{-4}).
[21] In the metallic phase limiting the FM phase, *weak* ferromagnetism has been observed using the DMRG method. For example, at $J/t = 1, x = 0.5$, the states with $S^z_{\text{total}} = 1$ and 0 are degenerate for $N \geq 12$ OBC clusters.
[22] Using DMRG the phase separation boundary is difficult to obtain due to large uncertainties in the data.
[23] V. J. Emery *et al.*, Phys. Rev. Lett. **64**, 475 (1990).
[24] S. Yunoki, J. Hu, A. Malvezzi, A. Moreo, N. Furukawa, and E. Dagotto (to be published).
[25] The AF correlation length ξ_{AF} for a $S = 1$ chain is large, about 6 lattice spacings. ξ_{AF} grows rapidly with S.
[26] C. H. Chen *et al.*, Phys. Rev. Lett. **71**, 2461(1993); S.-W. Cheong *et al.*, Phys. Rev. B **49**, 7088 (1994).